Sub-Cycle Ground Fault Location – Formulation and Preliminary Results

Charles J. Kim, *Senior Member, IEEE*, and Thomas O. Bialek, *Member, IEEE*

***Abstract*--A new time-domain approach of locating transitory, sub-cycle faults is introduced with a detailed formula derivation of the fault distance calculation for a single line-to-ground fault in the circuit of a substation, utilizing only the discrete voltage and current samples obtained at the substation. The formula is obtained from an equivalent circuit of the faulted circuit with voltage injection and the superposition principle using the parameters of net fault voltage and current. In addition to the fault distance, the approach also derives an equation which can produce the source reactance of the substation bus by the same parameters. The steps for implementing the derived formula in a practical application are illustrated, and then a preliminary test result with the actual substation measured data is discussed.**

***Index Terms*—Fault location, transitory faults, sub-cycle faults, intermittent fault, cable fault.**

I. Introduction

ELECTRIC utilities continuously look for ways to utilize technology to improve reliability by reducing the frequency and duration of customer outages. The integration of advanced fault location into operation systems including Supervisory Control and Data Acquisition (SCADA) and Outage Management System (OMS) will provide the ability to achieve greater reliability and reduce operating and maintenance expenses by quickly and accurately indicating both permanent and momentary faults, finding their location, shortening response time, and improving reliability indices. The accurate information on fault location eliminates the costly and time consuming fault chasing methods that stress system components exposed to fault currents.

Most fault location algorithms rely on phasor information of voltage and current in calculating line impedance or reactance as the main variable as fault distance [1 - 4]. The phasor is defined in and obtained from steady-state sinusoidal signal of voltage and current. Therefore, the fault location algorithms wait, after the on-set of the fault which without exception first manifests a transitory behavior, for the start of the steady-state period of fault signals and, using the steady-state sinusoidal signals of, for example, two or more cycles, calculate the magnitudes and phase angles of the signals to produce phasor information of the signals for the fault distance calculation [5- 6]. However, a great portion of faults, especially in underground cables, show their signature behaviors with not only without steady-state signals but also with fewer than 2 cycles of abnormal signal period before returning to normal signal pattern. Many, if not all, faults under this category manifest its abnormal signal behavior for 1 cycle or even ½ cycle period [7]. These types of faults are often called transitory or intermittent faults since they are not permanent faults but may be precursors of permanent faults to come. Therefore, the correct location of transitory intermittent faults is crucially important in prevention of faults and unscheduled outages. However, the conventional fault location algorithms cannot locate these types of faults.

Research efforts have been made in the last few years by the authors in the problem of locating transitory faults which last less than 2 cycles, aiming to locate even less than 1 cycle, sub-cycle, faults. The objective of this paper is to report the theory formulation and circuit modeling of the transitory fault location. The principle theory of transitory fault location combines the conventional injection method at the faulted location, which is to be determined, and the calculation of line inductance as the distance to the location using the voltage and current signals measured at the substation. The theory's main distinctive feature is that it does not need the inductances of the faulted, otherwise, healthy line or source, the essential information required by most of the fault location algorithms. Another important feature of the transitory fault location method is that the source impedance of substation transformer is obtained in the process of fault location calculation.

The sub-cycle fault location pursues time domain approach on the faulted circuit considering only reactive current and voltage ignoring resistance in the circuit and the load. This assumption is acceptably true to the actual measurement results of fault voltage and current. In formulating the fault distance in terms of the line inductance to the fault, the net fault voltage and current, which can be obtained by subtracting the nominal voltage and current from the fault voltage and current, respectively, over the time span of the transitory fault presence, are the major parameters in the calculation. The other important parameters are the voltage and the current at the fault inception time. On the circuit with the above parameters, a voltage injection method is applied with assumption that there is no fault resistance involved and thus, at the fault location, the voltage is zero. Then, the fault condition is represented by injecting the

C. J. Kim is with the Department of Electrical and Computer Engineering, Howard University, Washington, DC 20059 USA (e-mail: ckim@howard.edu).

T. O. Bialek is with San Diego Gas & Electric, San Diego, CA 92123 USA (e-mail: tbialek@semprautilities.com).

negative voltage at the fault inception time and, employing the superposition principle, only this voltage of fault inception is considered as the sole source in the faulted circuit of our interest, ignoring the main source, to calculate the distance to the fault using only the net fault voltage and current.

In the analysis and derivation of fault location formula, we follow the present practice and design of the substations of San Diego Gas & Electric (SDG&E) from which recordings are made and fault signals are obtained. In particular, the substation transformer(s) are Y-connected and direct grounded and a 3-phase capacitor bank is connected to the substation bus with options of ungrounded or grounded connection via a ganged switch. The substation measurement is conducted on the bus therefore the measured voltage is the bus voltage and the measured current is the current from the main source which may indicate the combined current from multiple circuits connected to the bus.

The sub-cycle faults are transitory and intermittent and they are mostly single line-to-ground faults, therefore, this paper focuses on sub-cycle single line-to-ground fault and its distance from the substation. In the fault location formulation, we simplified the scope by having only one circuit connected to the bus. Therefore the measured current is the sum of the current through the capacitor and that of the circuit, the details of which are illustrated in the sections to follow. Section 2 formulates single line-to-ground fault location, followed by section 3 which provides illustrated steps of implementing the formula in practical fault distance calculation. Then, section 4 describes the preliminary tests of the formula with actual substation data acquired from SDG&E. Section 5 concludes the paper with discussions and future works.

II. Single Line-to-ground Fault Location Formulation

A. Grounded Y-Connected Capacitor Bank Case

Let's start our discussion with a circuit diagram shown in Fig. 1 for a single line-to-ground fault on phase A and at the location x in the assumed substation and one circuit configuration.

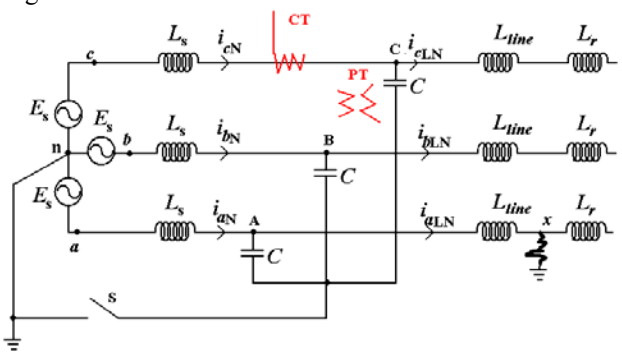

Fig. 1. Circuit Diagram for a Single Line-to-Ground Fault on Phase A.

The circuit is equivalently expressed with a sinusoidal source E_s with source inductance L_s, parallel capacitance C, inductance of the circuit from the substation to the location of the fault, L_{line}, and the inductance of the circuit from the fault location to the end of the circuit, L_r, with all resistive components ignored. The only variables measurable at the substation, through CTs and PTs, are the current flowing through the source impedance L_s and the bus voltage across the capacitor C. The approach intends to calculate the inductance L_{line} to x by using only the substation measured voltages and currents.

Now, let's assume that at time t=0, a phase A ground fault occurs at the location x with zero fault resistance. At that instant, the voltage at x becomes zero. The voltage zero incident can be represented as an injection of the negative voltage, $-v_{ax}(0)$, into the location x of the system. Also, since our interest is only in the change of voltage and current, termed "net fault voltage and net fault current" due to the fault, not in the total value by the injected voltage and the source voltage, we can deactivate the source voltage E_s from the equivalent circuit while keeping $-v_{ax}(0)$ between x and the ground. The circuit of injection and superposition principle now reduces the circuit diagram of Fig. 1 to the diagram of Fig. 2.

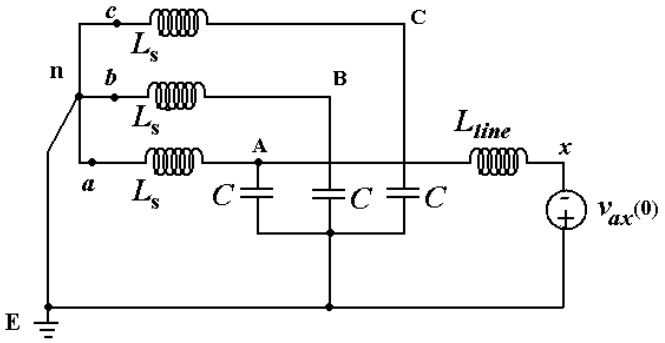

Fig. 2. Reduced Circuit Diagram of Single Line-to-Ground Fault with Voltage Injection and Superposition Principle.

By rearranging the circuit diagram of Fig. 2, we can eliminate the two branches of phases B and C, by the fact that they are shorted to the neutral and ground, and thus we have only phase A components of source inductance and capacitance, along with the line inductance to the fault, as illustrated in Fig. 3.

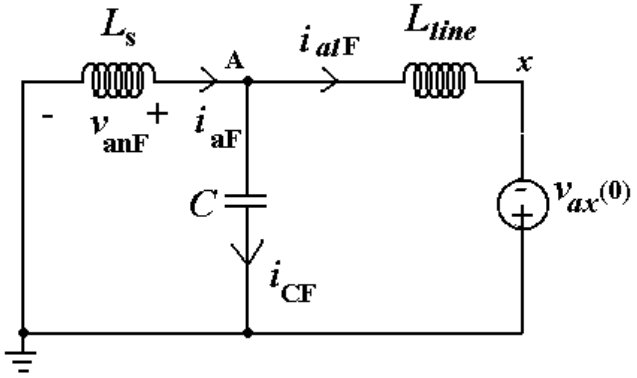

Fig. 3. Further Reduced Circuit Diagram of Fig. 2.

The currents of i_{aF}, i_{CF}, and i_{alF} and the voltage v_{anF} are the net fault currents and voltage, respectively. The net current i_{aF} and the net voltage v_{anF} can be obtained by subtracting the measured normal values from the measured values at fault. The only source in the circuit is the injected negative voltage whose magnitude is the same as the voltage at x just before the fault inception. Now, the problem is equivalent to the transient response with a DC voltage switched on to the circuit at t=0.

From Fig. 3, we can draw the following equations from the circuit:

$$i_{aF} = i_{alF} + i_{CF} \quad (1),$$

$$v_{anF}(t) = -L_s \cdot \frac{di_{aF}(t)}{dt} \quad (2), \text{ and}$$

$$v_{anF}(t) = L_{line} \cdot \frac{di_{alF}(t)}{dt} - v_{ax}(0) \quad (3).$$

Before we proceed further, there is one important discovery in equation (2): the source inductance value can be uniquely determined, at fault, by the net fault voltage divided by the rate of the net fault line current over the time as:

$$L_s = -\frac{v_{anF}(t)}{\frac{di_{aF}(t)}{dt}} \quad (4).$$

Then, combining equations (1) and (2) leads to the following net fault voltage equation:

$$v_{anF}(t) = -L_s \cdot \frac{di_{aF}(t)}{dt} = -L_s \cdot \frac{d}{dt}\left[i_{alF}(t) + i_{CF}(t)\right] \quad (5).$$

Equation (5) can be further reduced to the following equation:

$$v_{anF}(t) = -L_s \cdot \frac{di_{alF}(t)}{dt} - L_s \cdot C \cdot \frac{d^2 v_{anF}(t)}{dt^2} \quad (6).$$

By the way, equation (6) contains the differentiation of the net line fault current, which is not available from the substation measurement devices. By rearranging equation (3) with respect to the net line fault current, and substituting it with the net line fault current in equation (6) lead to the final fault distance inductance equation (7) with terms of the net voltage and current which are obtainable from the substation measured values:

$$L_{line} = \frac{v_{anF}(t) + v_{ax}(0)}{\frac{di_{aF}(t)}{dt} - C \cdot \frac{d^2 v_{anF}(t)}{dt^2}}. \quad (7)$$

The above distance to fault can be expressed in the dot notation form of a derivative:

$$L_{line} = \frac{v_{anF}(t) + v_{ax}(0)}{\dot{i}_{aF}(t) - C \cdot \ddot{v}_{anF}(t)} \quad (8)$$

In addition, as we already derived above, the source inductance can be expressed by

$$L_s = -\frac{v_{anF}(t)}{\dot{i}_{aF}(t)}. \quad (9)$$

The value of $v_{ax}(0)$ is the same as bus voltage $v_{an}(0)$ at the onset of fault, since there is no reactive current in the line. Alternatively, however, the value $v_{ax}(0)$ can be conveniently approximated to the value of the peak or negative peak value of the nominal phase voltage, because of the observation that the insulation breakdown of transitory or intermittent fault occurs at the maximum voltage point, positive or negative [7]. Of course, random faults or lower breakdown condition of insulation failure can occur at lower voltage magnitude than the peak value. When this non-peak insulation breakdown is more the norm than peak-voltage fault inception, using $v_{an}(0)$ would be the proper choice for the value of $v_{ax}(0)$.

B. Ungrounded Y-Connected Capacitor Bank Case

A phase A fault to ground at location x in case of ungrounded 3-phase Y-connected capacitor is illustrated in Fig. 4.

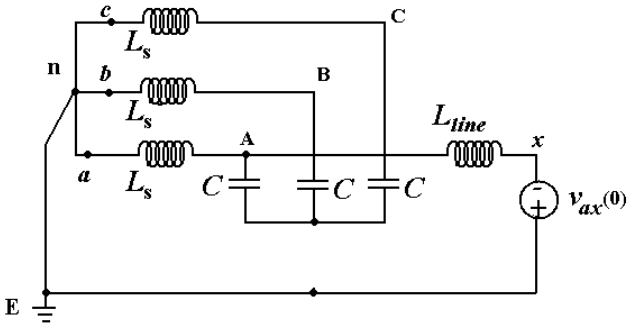

Fig. 4. Circuit Diagram of Single Line-to-ground Fault With Ungrounded Y-Connected Capacitor Bank.

The circuit diagram can now be rearranged and simplified to the equivalent circuit of Fig. 5 following the voltage injection and superposition principle.

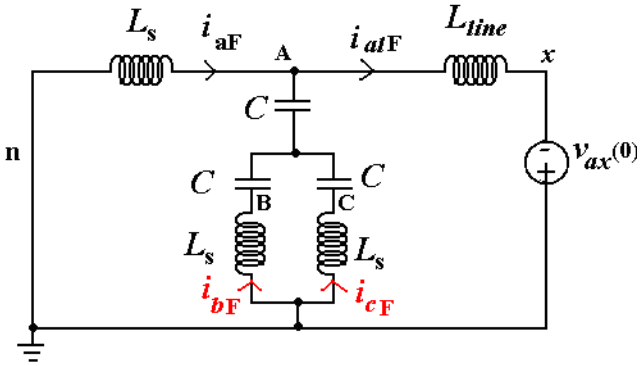

Fig. 5. Equivalent Circuit of Fig. 4.

With net fault currents of all three branches merging at a point in Phase A, as depicted in Fig. 5, it is apparent that the derivation of line inductance to the fault is simpler in ungrounded capacitor bank case. It is clear that from the combined branch, the combined net fault phase current from B and C flows into phase A to become the net fault line current. Since the sum of the three phase currents becomes the residual current, which is also available from the substation measurement, the net fault current is the same as the net fault residual current:

$$i_{alF}(t) = i_{aF}(t) + i_{bF}(t) + i_{cF}(t) = i_{rF}(t). \quad (10)$$

Therefore, from the voltage relationship at the node A of the circuit,

$$v_{anF}(t) = L_{line} \cdot \dot{i}_{alF}(t) - v_{ax}(0) = L_{line} \cdot \dot{i}_{rF}(t) - v_{ax}(0),$$

we can get the final fault distance equation for ungrounded Y-connected substation capacitor bank case:

$$L_{line} = \frac{v_{anF}(t) + v_{ax}(0)}{\dot{i}_{alF}(t)} = \frac{v_{anF}(t) + v_{ax}(0)}{\dot{i}_{rF}(t)}. \qquad (11)$$

C. No Capacitor Bank Case

How do the equations (8) and (11) change if there is no capacitor connected at the bus or if we ignore the capacitor in the formulation of the fault distance? The answer is hinged on the fact that i_{alf} is the same as i_{aF} when C=0 (see Fig. 5). Then, equations (8) and (11) provide the same equation of

$$L_{line} = \frac{v_{anF}(t) + v_{ax}(0)}{\dot{i}_{aF}(t)}. \qquad (12).$$

III. Implementation of Fault Location Formula

A. Description of the Data

Following the industry's significant interest in fault location, EPRI launched a multi-year base research program to evaluate different approaches, identify limitation, and develop recommendations as a function of types of system [8]. The program focused on the actual implementation of fault location functionality within power quality monitoring systems. The project helped to implement the latest fault location approaches within the PQView data management and analysis system and to assist with the integration with other systems that must be part of the fault location function – electrical database, GIS, and operational databases.

PQView is the premier industry tool for managing large databases of power system monitoring information. It is used by many utilities around the world as the foundation for collecting from a variety of different monitors, managing the database of disturbance and steady state data, reporting on performance, and providing alarms and notifications for problem conditions [9]. SDG&E, beginning in 1993, eight power quality monitors had been previously installed, and from 2005 a total of 40 power quality monitors integrated with PQView, called PQNode, has been installed as of 2007.

The PQnodes installed at the Creelman Substation from which the data for testing the sub-cycle fault location were obtained are Dranetz-BMI PQNode 8010 which captures triggered and periodic steady-state waveforms with simultaneous sampling rate of 128 points per 60Hz cycle for 3 phase voltages, 3 phase currents, and residual current. The PQnode installed at each of the two buses, North and South Buses, at the Creelman substation was set to record, with triggered record setting, 2 cycles of pre-triggered event waveforms and 12 cycles of post-triggered event. The trigger was set to respond to the voltage or current magnitude change of +/- 10% or more. The data collected from the PQnodes have been used to test the EPRI's fault location functionality applying the conventional impedance (or reactance) algorithm [9].

B. Computation Algorithm of the Fault Location Formula

From the fault distance formulation, we draw the following 3 equations for the fault distance in terms of the line inductance under different capacitor bank connection configurations: $L_{line} = \frac{v_{anF}(t) + v_{ax}(0)}{\dot{i}_{aF}(t) - C \cdot \ddot{v}_{anF}(t)}$ (8) for grounded Y-connected capacitor bank,

$L_{line} = \frac{v_{anF}(t) + v_{ax}(0)}{\dot{i}_{alF}(t)} = \frac{v_{anF}(t) + v_{ax}(0)}{\dot{i}_{rF}(t)}$ (11) for ungrounded Y-connected capacitor bank, and

$L_{line} = \frac{v_{anF}(t) + v_{ax}(0)}{\dot{i}_{aF}(t)}$ (12) for no capacitor bank.

It is apparent that application of the formula needs (i) net fault voltage and current, (ii) the voltage at fault inception, and (iii) the first discrete derivative of the net fault current and the second discrete derivative of the net fault voltage. This section describes the steps to be taken to derive the necessary discrete values and the process of applying the formula for the distance to fault at each sample point of the captured data.

Step 1: Raw Data from PQView

The first step of the process is to read the captured raw data which contains at least 1 cycle of normal and several cycles of post-disturbance waveforms of voltages and currents. Fig. 6 is one example of such waveforms which, for clear display purpose, depicts only phase B voltage, scaled down by 5, and current and residual current.

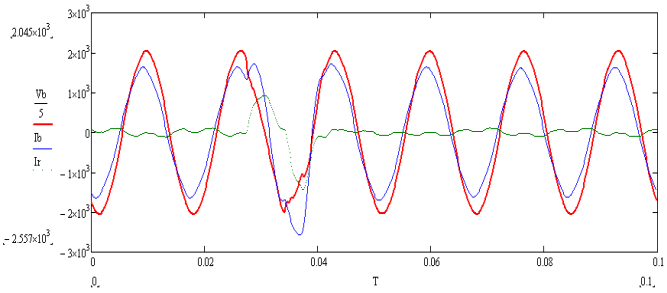

Fig. 6. An example raw data of Phase B to ground fault (Phase voltage (Vb), phase current (Ib), and residual current (Ir)).

Step 2: Net Fault Value Derivation

Separated by the fault inception time stamp, the captured raw data of voltage and current are to be split into two data components: Synchronized pre-fault data and post-fault data of a full cycle length or more. Synchronization of both data sets is very important because the former is subtracted from the latter for the net fault value. The synchronization is established in the following manner. First, the normal data over the entire captured data length can be obtained by getting a full cycle of pre-fault samples, starting from the first sample point to the 128th sample to cover one complete normal cycle, and then by concatenating the same 1 cycle after the full cycle pre-fault samples repeatedly until the combined sample

number is the same as that of the captured raw data. Second, the entire captured raw samples, including the 1 cycle pre-fault normal sample in the beginning, are used as the fault data.

Then, the net fault data are obtained by subtracting the normal data from the fault data, sample by sample. The graph in Fig. 7 depicts the net phase B fault voltage, net phase B fault current, and net residual fault current, obtained from the raw data of Fig. 6. On the other hand, the value of voltage at the fault inception time becomes the initial phase voltage $v_x(0)$, the negative of which is the injected voltage source in the injection and superposition analysis we performed in the previous section.

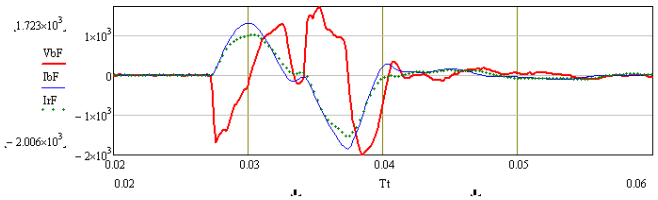

Fig. 7. Net Fault Voltage (VbF) and Current (IbF) of Phase B and residual Current (IrF) of the Raw Data of Fig. 6.

Step 3. Determination of Fault Inception Time

The fault inception time may be obtained by the PQnode and PQView by utilizing the triggered recording setting for data storage. Or it can be obtained by using the sample number at which both (either) the net fault current over a certain threshold value and (or) the net fault current under a threshold. From Fig. 7 net fault voltage and current waveforms, the fault inception time is not difficult to pinpoint.

Step 4: Differentiation of Net Fault Current/Voltage

The formula for fault distance and the source inductance contain the first derivative of the net fault current and, for grounded capacitor bank configuration, the second derivative of the net fault voltage. How we obtain the first derivative from sampled data is explained here. Generally, the numerical differentiation of digitized signals can be derived from the definition that the first derivative (dy/dt or $\dot{y}$) of a time varying signal (y) is the rate of change of y with time *t*, which is interpreted as the slope of the tangent to the signal at each point. Under the constant and identical time interval (Δt) between adjacent sample points, which is 0.13 [ms] in our case, the simplest algorithm for computing a first derivative at sample time *n*, termed as the first order forward difference formula for first derivative, is expressed by:

$$\dot{y}_n^1 = \frac{y_{n+1} - y_n}{\Delta t} \qquad (13).$$

By applying Taylor expansion, a second order centered difference formula for the first derivative is obtained by:

$$\dot{y}_n^2 = \frac{y_{n+1} - y_{n-1}}{2\Delta t} \qquad (14).$$

Further, the fourth order approximation of the first derivative is expressed by:

$$\dot{y}_n^4 = \frac{y_{n-2} - 8y_{n-1} + 8y_{n+1} - y_{n+2}}{12\Delta t} \qquad (15).$$

For the data we tested, the second order first differentiation was the best choice due to reduced sensitivity to the random, white noise components contained in the raw data. However, this may not be true for other cases. Therefore, a proper discrete derivative order must be selected case by case. In summary, the first derivative of the net fault current can be determined at each sample point by applying the numerical differentiation formula. Fig. 8 illustrates the first derivatives of the net fault voltage, current, and residual current, respectively.

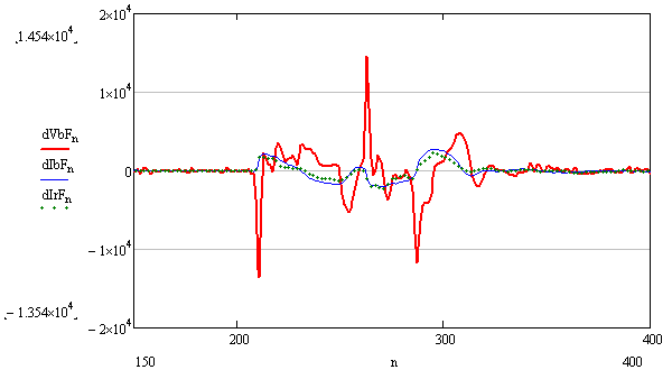

Fig. 8. The first derivative waveforms of phase B net fault voltage (dVbF), current (dIbF), and residual current (dIrF), respectively.

Step 4: Second Differentiation of Net Fault Voltage

Even though there are many ways to obtain the second derivative of the net fault voltage, we choose to use the above first derivative twice. Fig. 9 depicts the net fault voltage, first derivative of the net fault voltage, and the second derivative of the net fault voltage, all of phase B.

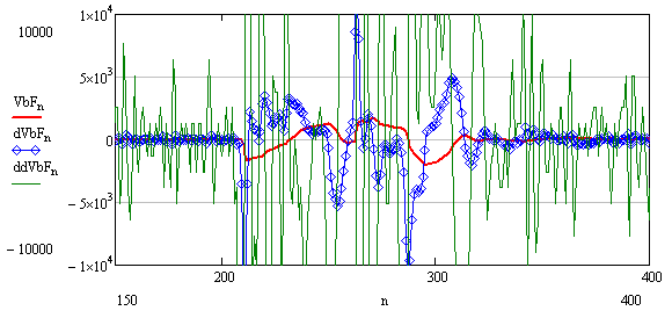

Fig. 9. Net fault voltage (VbF), first derivative of the net fault voltage (dVbF), and the second derivative of the net fault voltage (ddVbF) of phase B.

Step 5: Formula Execution and Output Generation

With the necessary parameters produced in the above steps, the formula for sub-cycle fault location can be executed. Note that in the normal situation, since the net fault voltage and net current or its derivative are close to zero, the output of the formula would produce infinity or indeterminate distance to fault. Therefore, in the process of the calculation, if the net fault value is zero, the process should stop to avoid "divide by zero" error. Alternatively, if the net fault value is near zero, make the output a small number to produce the distance with a big number so that the result would be ignored and referred as no-fault situation. In our calculation, we adopt, for both the source inductance and the fault distance inductance calculations, this alternative approach, which results in very

spiky output of inductance in a normal condition. However, in faulted condition, they both have consistent values.

As stated above, the calculation is on the digitized data and, therefore, the output is produced at each sampling point. Due to the use of the first and second derivatives, the output could be very sensitive to noise in the waveform. However, the tests reveal that there is a certain period in which the values of the formula are maintained with consistency, however short the period may be. In the case of source inductance which does not involve second derivative, the stabilized period is long enough to not obscure the determination of the value. In both cases, the results are determined as the values of stabilized periods. Therefore, we have to wait until enough number of sampling points is considered and a trajectory of the final output is obtained so that, from the trajectory, the minimum and stabilized value would be selected as the final output value. In the experimentation, about quarter cycle or half cycle would be enough to produce stabilized trajectory for determining the lowest value produced.

Fig. 10 illustrates the sample by sample calculated result of the fault distance in reactance, converted with 60Hz power frequency and derived distance inductance, with spiky regions of normal period and periodic consistent and stabilized values after the fault inception. If the calculated fault distance of stabilized periods may have different values as in Fig. 10, we decide to pick the first stabilized value after the fault inception as the fault distance since the transient right after inception time contains the initial faulted circuit information while the subsequent values may have resulted from changed circuit condition or reflections however minor or short-lived they may be. Following this pick-the-first stabilized value, the fault distance in the figure is 5 ohm.

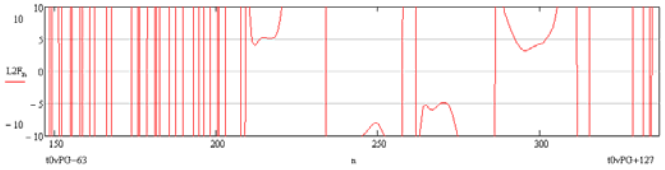

Fig. 10. Example Fault Distance in Reactance (L2F).

IV. Preliminary Test with Substation Measured Data

In addition to the power quality monitoring in SDG&E, an outage listing per circuit of all substations has been produced with outage IDs, causes, isolating and or damaged devices, and occurrence time stamps. To collect testing data for the developed sub-cycle fault location formula, we studied the outage listing for year 2006 and collected only single line-to-ground faults with cable damage caused outages at the Creelman substation. Then, we downloaded the captured data from the PQnode, which closely matched the cable damage outages but lasted less than 2 cycles, for the substation via PQView data management system. The data we finally obtained from PQView, only four outage events, were always slightly ahead in time of the cable damaged outage in the listing, clearly revealing that the sub-cycle fault was not captured by clearing devices but, once self-cleared, then proceeded to a permanent fault. All four faults occurred in the same circuit (circuit #973), and the distance to each of the faults was given as the distance in miles from the bus to the fault location. The four outage events are summarized in Table I, and their waveforms in phase voltage (scaled down by 10), phase current, and residual current are shown in Fig. 11.

TABLE I
Summary of the Four Outage Events

Event No	Fault Phase	Occurrence	PQnode file ID	Cause	Distance [mi]
1	C	05/06/06 14:55	050606-164307	Cable Rack	4.08
2	C	05/15/06 06:16	051506-014738	UG Cable	1.93
3	B	08/21/06 09:35	082106-014936	UG Cable	5.02
4	C	12/15/06 21:41	121506-194504	UG Cable	5.02

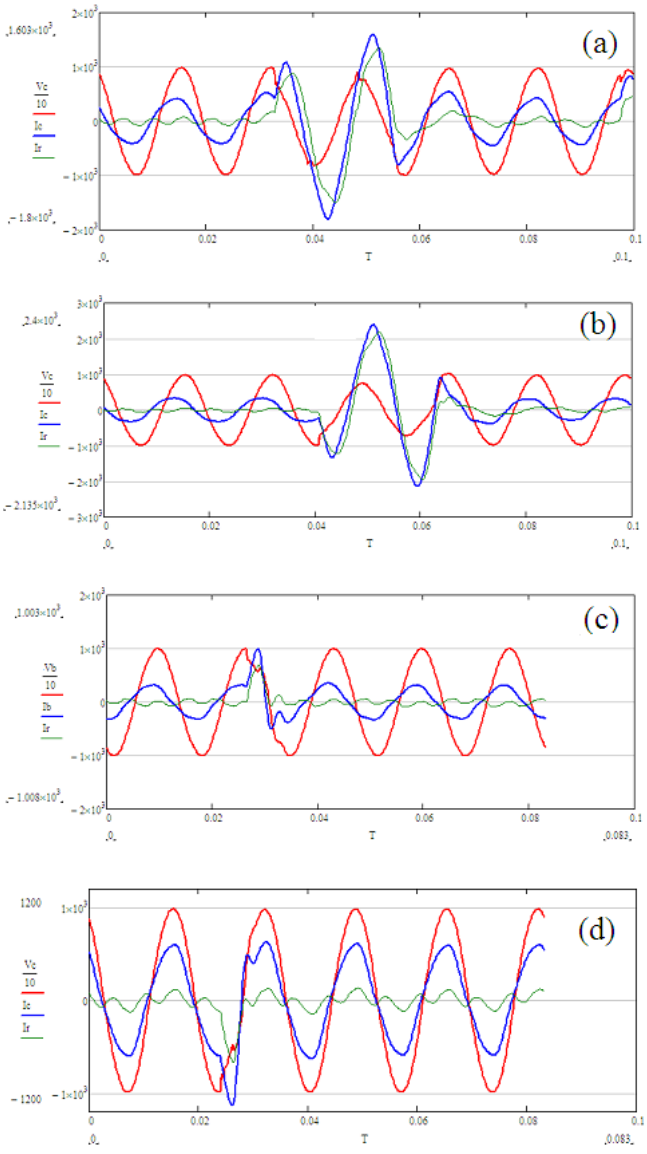

Fig. 11. Waveforms of the four events, 1 to 4, from top to bottom.

The preliminary test results are shown in Fig. 12 (for source inductance) and Fig. 13 (for fault distance). Fig. 12 shows the source inductance in sample by sample values for

each of the 4 events, and with the reactance values 1.15, 1.15, 1.24, and 1.18, we can conclude that the source inductance formula and its result during sub-cycle faults are consistent.

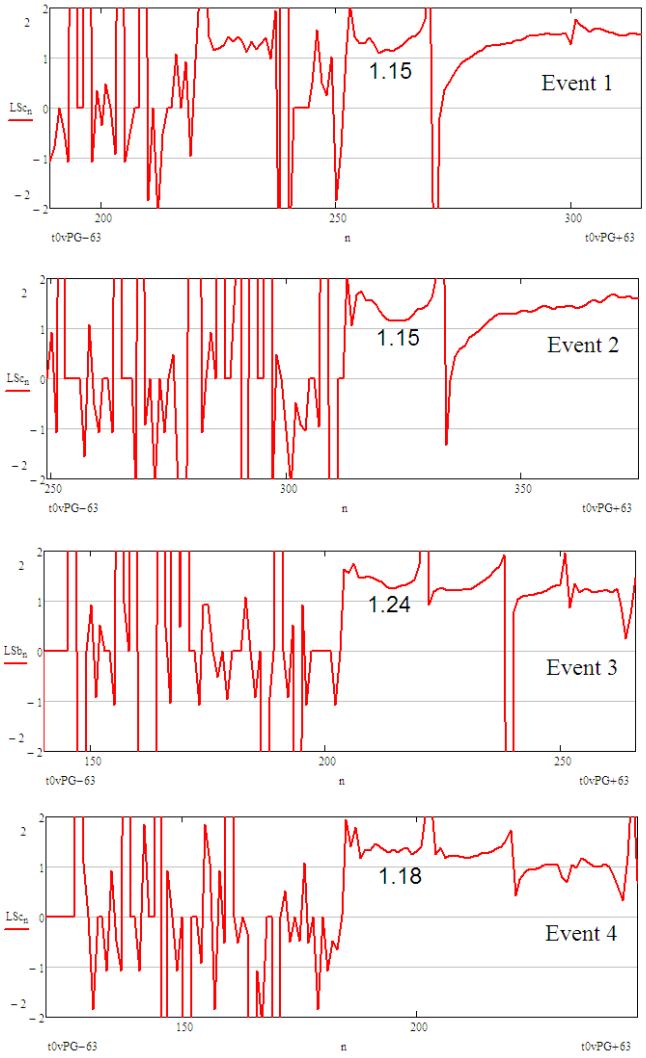

Fig. 12. Source Impedance values of the 4 events.

Fig. 13 shows the results of fault distance in reactance for each of the four events. Since the fault distance calculation of the approach produces reactance values, the direct comparison with the actual events' distances in mile is difficult. However, it is clear that the same distanced events of 3 and 4 do not produce the same reactance values (5.33 for event 3 and 6.82 for event 4). Also, even though the farther distance fault of event 1 has bigger reactance value (4.34) than that of event 2 (3.34), it is not clear if there is any linear relationship in the reactance values to the distance in mile.

We plot a graph of the calculated fault distance in reactance versus the outage list indicated fault distance in mile (Fig. 14) to see if we can draw relationship between the two and to assess the validity of the fault distance formula developed in the paper. Events 1 and 3 are on the slope 1 linear line, while events 2 and 4 are above it. With only 4 events alone, it is premature if there is any established relationship between two, linear or logarithmic, or it will turn out to be no relationship at all after enough number of event analyses. Again, this paper is only for preliminary test, and, definitely, more tests with actual data are to be performed. Also, improvement of the formula, inclusion of fault resistance for instance, would be considered in the future work. However, as in the source inductance, there is some hint that the developed formula would produce, in the long run, consistent fault distance values.

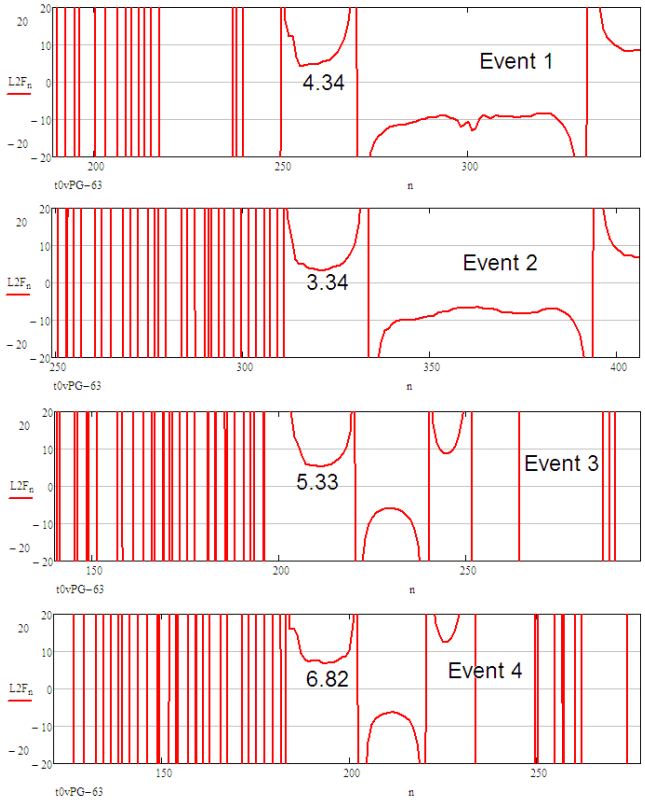

Fig. 13. Fault Distance for each of the four events.

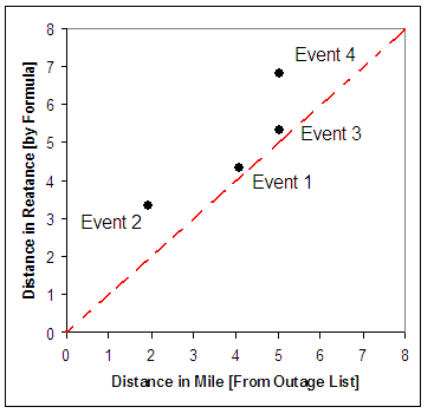

Fig. 14. Relationship between the fault distance in mile and the calculated fault distance in reactance of the four events.

V. Conclusions

This paper reported the theory formulation and circuit modeling of sub-cycle transitory fault location by employing the conventional injection method at the faulted location and the superposition principle to calculate the line inductance to the fault as the distance using only the voltage and current

signals measured at substation. The main distinctive feature of the fault distance formula is that it does not need the inductances of the line or sources. Another important feature of the transitory fault location method is that the source impedance of substation transformer is obtained in the process of fault location calculation. The detailed steps and processes of the formula for practical application was detailed along with preliminary test results with four actual sub-cycle faults involved in underground cable and the cable rack. There was consistency in the calculated values of the source inductance among the events, however, the relationship between the calculated reactance to fault and the given fault distance in mile, given in the outage listing, was not clearly determined due to only few number of outages. More testing and improvement of the formula would have to be paralleled to have better assessment of the validity of the proposed formula for fault distance of sub-cycle faults.

VI. References

[1] E. Schweitzer, "A Review of Impedance-Based Fault Locating Experience," *Proceedings of the 15th Annual Western Protective Relay Conference*, Spokane, WA, October 24-27, 1988.

[2] D. Novosel, D. Hart, E. Udren and J. Garitty, "Unsynchronized two-terminal fault location estimation", *IEEE Trans. on Power Delivery*, Vol. 11. No. 1, Jan. 1996, pp. 130-138.

[3] T. Takagi, Y. Yamakoshi, M. Yamaura, R. Kondow and T. Matsushima, "Development of a new type fault locator using the one-terminal voltage and current data", *IEEE Trans. On Power Apparatus and Systems*, Vol. PAS-101, 1982, pp. 2892-2898.

[4] A. Wiszniewski, "Accurate fault impedance locating algorithm", *IEE Proceedings*, Part C, Vol.130, No.6, 1983, pp. 311-315.

[5] E. Schweitzer and J. Roberts, "Distance Relay Element Design," *19th Annual Western Protective Relay Conference*, Spokane, Washington, October 20-22, 1992.

[6] C. Kim, Lecture Notes on Fault Detection and Location in Distribution Systems, June 2010.

[7] L. Kojovic and C. Williams, "Sub-cycle detection of incipient cable splice faults to prevent cable damage," *Proc. IEEE Power Engineering Society Summer Meeting*, 2000. Vol. 2, pp. 1175 – 1180. 16 Jul 2000 - 20 Jul 2000. Seattle, WA , USA.

[8] M. McGranaghan, "Development and Demonstration of Advanced Monitoring Systems for Fault Location, Analysis, and Prediction," DOE Annual Program and Peer Review Meeting, San Ramon, CA. May 25-26, 2006.

[9] M. McGranaghan, T. Short, D. Sabin, "Using PQ Monitoring Infrastructure for Automatic Fault Location," *Proceedings 19th CIRED*, 21-24 May. 2007.

VII. Biographies

Charles Kim (M'90, SM'06) received a Ph.D. degree in electrical engineering from Texas A&M University (College Station, TX) in 1989. Since, 1999, he has been with the Department of Electrical and Computer Engineering at Howard University. Previously, Dr. Kim held teaching and research positions at Texas A&M University and the University of Suwon. Dr. Kim's research interests include failure detection, anticipation, and prevention in safety critical electrical/electronic systems in power, aerospace, and nuclear industries.

Thomas Owen Bialek (M'82) received a B.Sc.(EE) and M.Sc.(EE) from the University of Manitoba in 1982 and 1986 respectively. He also obtained a Ph.D. in Electrical Engineering from Mississippi State University in 2005. He is currently employed by San Diego Gas & Electric Company ("SDG&E") as a Chief Engineer on the Smart Grid Team. His present responsibilities involve smart grid strategy and policy for transmission and distribution issues including equipment, operations, planning, distributed generation and development of new technologies.